Quadrature Imbalance Compensation Algorithms for Coherent PDM QPSK Systems

C. S. Petrou[(1)], A. Vgenis[(1)], I. Roudas[(1)] and L. Raptis

(1)Dpt. of Electrical & Computer Engineering, University of Patras, Rio, 26500, Greece; E-mail: petrou@ece.upatras.gr

Abstract: We compare three quadrature imbalance compensation algorithms for coherent PDM-QPSK systems, including a novel, blind, adaptive equalizer. We show that dedicated quadrature imbalance compensation is mandatory and cannot be performed by regular distortion mitigating equalizers.

1. Introduction

Coherent phase-diversity receivers suffer from quadrature imbalance (QI) [1],[2]. QI arises from imperfections of the 90° optical hybrid, regardless of the hybrid type, and from responsivity mismatches, in both balanced and single-ended photodetectors. It is a ubiquitous effect that affects the performance of all subsequent DSP algorithms at the receiver [3]. In this paper, we propose a novel, blind, adaptive QI compensation scheme, suitable for polarization division multiplexed (PDM) quadrature phase shift keying (QPSK) systems, based on the constant modulus algorithm (CMA) [4]. We study the robustness of the proposed QI compensator in the presence of amplified spontaneous emission (ASE) noise and quadrature amplitude and phase mismatch. Finally, we compare its performance with that of already proposed QI compensation algorithms [3], [5], using Monte Carlo simulation for bit error rate (BER) estimation, in a PDM QPSK system. We show that dedicated QI compensators are mandatory and cannot be substituted by common electronic equalizers, e.g. [6], used for distortion mitigation.

2. QI equalization schemes

The photocurrents at the output of a phase diversity receiver, after timing alignment, assume the form

$$\mathbf{I}=\left[I_{ip}\cos\left(a(t)+\varepsilon\right)\quad I_{qp}\sin\left(a(t)-\delta\right)\right]^{T},\qquad(1)$$

where I_{ip},I_{qp} are the I/Q photocurrent amplitudes, respectively, $a(t)=2\pi f_{IF}t+\Delta\varphi_n+\varphi_k$ is the instantaneous phase, f_{IF} is the intermediate frequency (IF) offset between the transmitter and LO, $\Delta\varphi_n$ is the difference between the laser phase noises, φ_k is the modulation phase, ε,δ are the phase deviations of the quadratures, and T denotes transposition. In (1), we omitted, for simplicity, the DC components of the photocurrents, the additive noise, the cross polarization interference due to polarization rotations, and other transmission effects. After sampling at the center of the symbol period T_S, relation (1) can be rewritten in matrix form, as $\mathbf{I}=\mathbf{M}\mathbf{I}_{\mathbf{Q}}$, where $\mathbf{I}=\left[I[n]\quad Q[n]\right]^{T}$ is the received photocurrent vector, $\mathbf{I}_{\mathbf{Q}}=\left[\cos a[n]\ \sin a[n]\right]^{T}$ is the desired quadrature component vector, and $\mathbf{M}$ is a mixing matrix representing the effect of QI. The proposed algorithm attempts to adaptively estimate $\mathbf{M}^{-1}$, using an iterative procedure, based on the CMA [4]. To facilitate convergence, we impose constraints on the elements of $\mathbf{M}^{-1}$

$$\mathbf{M}^{-1}=\begin{bmatrix}I_{ip}^{-1}\cos\delta & I_{qp}^{-1}\sin\varepsilon\\ I_{ip}^{-1}\sin\delta & I_{qp}^{-1}\cos\varepsilon\end{bmatrix},\qquad(2)$$

(Constrained QI-CMA). The CMA is used to estimate the parameters $\hat{I}_{ip},\hat{I}_{qp},\hat{\varepsilon},\hat{\delta}$, by minimizing the cost function $\xi[n]=e^{2}[n]$, where $e[n]=\mathbf{I}_{\mathbf{Q}}^{\mathrm{T}}[n]\cdot\mathbf{I}_{\mathbf{Q}}[n]-R$ is the error function and R is the sum of the average signal and noise powers. We define the auxiliary array of estimated parameters $\mathbf{Z}[n]=\left[I_{ip}[n]I_{qp}[n]\varepsilon[n]\delta[n]\right]^{\mathrm{T}}$, and use the stochastic gradient algorithm for their update

$$\mathbf{Z}[n+1]=\mathbf{Z}[n]-\mu\left[\frac{\partial\xi[n]}{\partial I_{ip}}\frac{\partial\xi[n]}{\partial I_{qp}}\frac{\partial\xi[n]}{\partial\varepsilon}\frac{\partial\xi[n]}{\partial\delta}\right]^{T},\qquad(3)$$

where μ is the algorithm step-size parameter. Further constraints can be introduced, i.e., $\lambda=\sqrt{I_{ip}/I_{qp}}$, $\varepsilon=0$, in order to decrease the number of independently adjustable parameters. However, this would result in a small additional penalty, as shown in the next section.

3. Results and discussion

We implement the PDM QPSK system shown in Fig. 1, in which 2×4 90° optical hybrids and balanced photodetectors (BPDs) are used. The photocurrents are initially passed through a DC block (DCB) and filtered by a low-pass filter (LPF) Then, they are sampled at the symbol rate and fed into an application specific integrated circuit (ASIC) for digital signal processing. In the ASIC, the QI is estimated separately for each phase-diversity receiver. Subsequently, the two quadratures are combined into a complex photocurrent and polarization demultiplexing (POLDEMUX) is performed [6]. IF offset estimation and phase tracking are performed using feedforward frequency (FFF) [7] and phase (FFP) [8] algorithms, respectively. Fig. 2 shows the OSNR penalty as a function of various settings of the optical hybrid and BPDs, when no QI compensation is performed. The OSNR penalty is calculated using a semi-analytical method [9] for a single polarization tributary, at

978-1-4244-3681-1/09/$25.00 ©2009 IEEE

$P_e=10^{-9}$. Penalties can routinely exceed 3 dB, even for relatively small deviations from the nominal settings. Non-ideal output couplers affect system performance less than non-ideal input couplers. Using any of the algorithms described in [3], [5] , the OSNR penalty, for all cases depicted in Fig. 2, is reduced below 0.3 dB. Subsequently, we evaluate the BER vs. OSNR. We set the phase mismatch of the phase diversity receivers to ±30°, the 3-dB coupler coupling coefficients to +30% of their nominal value, and the I/Q responsivity ratio deviation to 20%. We also assume a 500 kHz total 3-dB laser linewidth and a 5% $(T_S)^{-1}$ IF offset, which are typical values in practical systems. Finally, we include an arbitrary polarization rotation. Fig. 3(a)-(d) show representative constellations at the input (a), output of the polarization demultiplexer ((b) (d)), and after phase tracking ((c), (e)), with and without QI compensation, respectively, for an OSNR equal to 22 dB. Fig. 3(f) shows the BER vs. OSNR for a variety of cases. Dotted curves correspond to the case where no dedicated QI compensation is performed, but instead multitap butterfly equalizers [6] are used. Although the latter are successful in mitigating transmission effects, such as PMD, they are inadequate for compensating for large amounts of QI. This is intuitively understood since the transverse filter at each butterfly branch can not unravel the erroneous complex superposition of the two quadratures at its inputs. It is worth noting that an increase in the number of equalizer taps further deteriorates the performance, since a larger number of erroneous input samples with QI are added in the equalizer. The almost identical performance of algorithms [3], [5] and the proposed QI compensator stems from their similar operating principles, i.e., they are all zero-forcing equalizers that differ only in the accuracy of the estimation of the mixing matrix $\mathbf{M}$. Two other implementations of the constrained QI-CMA are also depicted in Fig. 3(f), with two ($\lambda,\delta,\ \varepsilon=0$) and three ($\lambda,\delta,\varepsilon$) adjustable parameters, respectively. They exhibit a small penalty compared to the case of four adjustable parameters, in favor of DSP simplicity. We note that, in implementing [5], time averaging over block sizes as small as 128 symbols suffices. Increasing the number of symbols changes the performance by less than 0.1 dB.

4. Conclusions

We compared the performance of two previously proposed QI compensation schemes and of a novel, blind, adaptive QI compensation algorithm. We conclude that QI can cause significant OSNR penalty and needs a dedicated compensation module. Common adaptive electronic equalizers cannot efficiently compensate for QI.

References

[1] U. Koc et al., OFC, OThI1, Anaheim, CA, Mar. 2006.
[2] I. Roudas et al., LEOS-ST., MA3.4, Portland, OR, Jul. 2007.
[3] C. Petrou et al., LEOS, TuFF3, New. Beach, CA, Nov. 2008.
[4] D. Godard, Trans.Comm., vol. 28, pp. 1867–1875, Nov. 1980.
[5] I. Fatadin et al., Phot.on. Technol. Lett., vol. 20, pp. 1733–1735, Oct. 2008.
[6] S. Savory et al., Opt. Ex., vol. 15, pp. 2120–2126, Mar. 2007.
[7] M. Morelli and U. Mengali, European Trans. on Telecommun., vol. 9, no. 2, pp. 103–116, March/April 1998.
[8] A. Viterbi and A. Viterbi, *IEEE Trans. on Inform. Theory*, vol. IT-29, no. 4, pp. 543–551, July 1983.
[9] M. Jerucim, *IEEE J. Select. Areas Commun.*, vol. 2, no. 1, pp. 153–170, Jan. 1984.

This research project is sponsored by the European Social Fund (75%) and the Greek Development Ministry (25%).

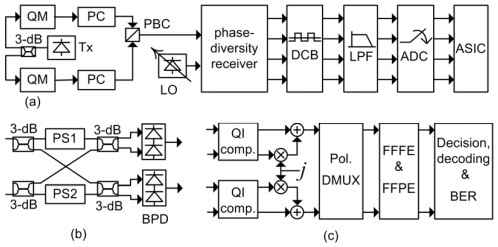

Fig. 1: System block diagram. (a) Transmitter and receiver; (b) 2×4 90° optical hybrid; (c) ASIC.

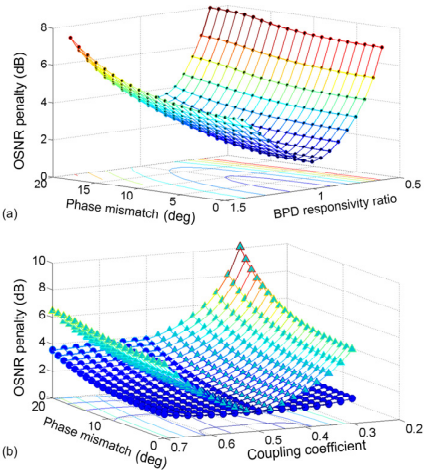

Fig. 2: OSNR penalty at error probability 10^{-9} for various settings of the optical hybrid and BPDs. (a) Combination of phase mismatch and BPD responsivity ratio deviation; (b) Combination of phase mismatch and coupling coefficient values (Circles: Non-ideal output couplers, Triangles: Non-ideal input couplers).

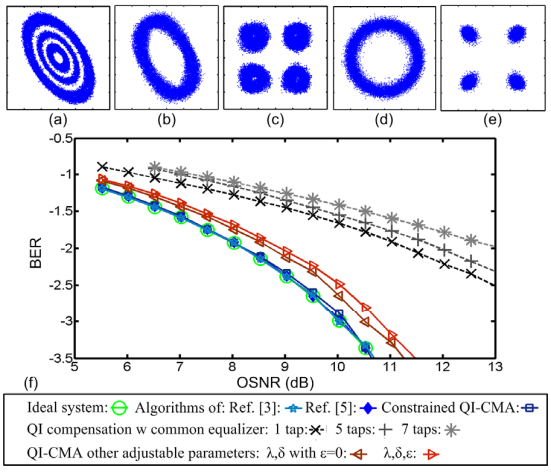

Fig. 3. Representative constellations: (a) input; (b), (d) at the output of the POLDEMUX and (c), (e), after phase tracking, with and without QI compensation, respectively; (e) BER vs OSNR.